

On the Tail of the Overlap Probability Distribution in the Sherrington–Kirkpatrick Model

Alain Billoire

Service de Physique Théorique, CEA/DSM/SPhT

Laboratoire associé au CNRS

CEA-Saclay, 91191 Gif-sur-Yvette cédex (France)

Silvio Franz

ICTP, Strada Costiera 11, PO Box 563

34100 Trieste (Italy)

Enzo Marinari

Dipartimento di Fisica, SMC and Udr1 of INFM and INFN

Università di Roma *La Sapienza*

P. A. Moro 2, 00185 Roma (Italy)

billoir@sph.t.saclay.cea.fr

franz@ictp.trieste.it enzo.marinari@roma1.infn.it

December 2, 2024

Abstract

We investigate the large deviation behavior of the overlap probability density in the Sherrington–Kirkpatrick model from several analytical perspectives. First we analyze the spin glass phase using the coupled replica scheme. Here generically $\frac{1}{N} \log P_N(q) \approx -\mathcal{A} ((|q| - q_{EA})^3)$, and we compute the first correction to the expansion of \mathcal{A} in powers of $T_c - T$. We study also the $q = 1$ case, where $P(q)$ is known exactly.

Finally we study the paramagnetic phase, where exact results valid for all q 's are obtained. The overall agreement between the various points of view is very satisfactory. Data from large scale numerical simulations show that the predicted behavior can be detected already on moderate lattice sizes.

1 Introduction

Although the solution of the Sherrington–Kirkpatrick (SK) model was proposed more than two decades ago [1], its physical interpretation is (now) quite clear [2], and one can try to answer to sophisticated questions in the framework of replica mean field theory [3], some fundamental aspects of the model are still poorly understood. Just to quote some recent works we are thinking here about the problem of time scales in the model [4], and to the question of chaos with respect to temperature variations [5, 6].

A further problem of interest concerning the SK model is the large deviation behavior of the order parameter probability distribution $P_N(q)$. In the usual mean field approximation the probability distribution of the order parameter $P_N(m)$ is obtained from the free energy, by considering it as a function of the order parameter. This approach cannot be pursued in the *replica approach*, since the free energy obtained when using the replica method has no physical interpretation for values of the parameter different from the saddle point [2]. A method to compute $P_N(q)$ in the Replica approach was proposed in [3], and used in [7], [8]. It amounts to apply the replica trick to two identical copies of the system, while imposing a constrained value of the overlap q . One finds that

$$\frac{1}{N} \log P_N(|q| > q_{EA}) = -\mathcal{A}(|q| - q_{EA})^3 + \mathcal{O}\left((|q| - q_{EA})^4\right) ,$$

where q_{EA} is the Edwards–Anderson order parameter (the maximum value allowed for the overlap in the infinite volume limit), and the proportionality coefficient was computed in [3] to zeroth order in $\tau = (T_c^2 - T^2)/2T_c$. Here we present results of a computation to the next order, and compare this prediction with numerical results obtained from a large scale simulation, using the parallel tempering algorithm. For $T \geq T_c$ we present the results of an exact calculation, in the replica symmetric scheme, that is limited neither to small q 's nor to the vicinity of T_c . This calculation corroborates nicely the other results.

There are somehow three main points in what we do here. At first we present a mean field computation that is based on coupling two replicas. This is in some sense a *sophisticated* computation, in which it is based on modifying the standard mean field theory (by coupling two replicas) to evaluate the rare fluctuations that determine the tail of $P(q)$. Here multiple checks are indeed very important. This is why, together with our computation, we present a numerical check of the result, that turns out to give very positive results. The third point is a byproduct of the second, and is in checking how much of the infinite volume physics (at low temperatures, in the broken spin glass phase) is already encoded in the sizes we can effectively study on our nowadays state of the art computers (up to $N = 4096$ in the present case): we will see that, as far as the present computation is concerned, things do work well, and we are moving on solid ground.

2 Large Deviations in $P(q)$ for $|q| > q_{EA}$

In this section¹ we sketch the main steps and give the results of our computations of the function $P_N(q)$ in the large deviation regime, i.e. for $|q| > q_{EA}$, for both $T < T_c$ and $T > T_c$.

It is well known that in the thermodynamic limit the disorder average of $P_{N,J}(q)$ is non-vanishing² in the interval $[0, q_{EA}]$, while sample to sample fluctuations remain strong even for large systems, in the infinite volume limit [2]. The probability of the complementary interval, i.e. of events with $q > q_{EA}$, is exponentially small in the system size [3]. For typical samples one has that, independently of the disorder realization,

$$P_{N,J}(q) \approx P_N(q) \propto \exp(-\beta N \Delta F(q)) , \quad (1)$$

where $\beta = \frac{1}{T}$ and $\Delta F(q)$ is the self-averaging free energy cost for keeping two replicas at a mutual overlap q :

$$\Delta F(q) = -\frac{T}{N} \log \overline{\left(\frac{1}{Z^2} \sum_{\{\sigma_i, \tau_i\}} e^{-\beta(H(\sigma) + H(\tau))} \delta(q - \frac{1}{N} \sum_i \sigma_i \tau_i) \right)} . \quad (2)$$

¹In the following we will take, without loss of generality, $q > 0$ (thinking for example to the application of an infinitesimal magnetic field).

²We assume that our starting Hamiltonian is symmetric under global spin reversal, and, as we already said, we restrict our averages to the $q > 0$ sector by using, for example, an infinitesimal magnetic field.

Here with the over-bar we have denoted the disorder average. One possible scenario would be such that the fluctuations of $\overline{P_{N,J}(q)}$ are dominated by rare (i.e. having exponentially vanishing probability) samples, causing $\overline{P_{N,J}(q)}$ to be different from $P_N(q)$: we will discuss this issue by comparing to numerical simulations in the next section.

In reference [3] the computation of $\Delta F(q)$ has been performed by using the method of *coupled replicas*: the computation of $\Delta F(q)$ for the SK model close to T_c , in the glassy phase $T < T_c$, has established that, in the lowest order in both $\tau \equiv (T_c^2 - T^2)/2T_c$ and $q - q_{EA}$, $\Delta F = \frac{1}{6}(q - q_{EA})^3$.

Let us start with the case $T < T_c$, and perform the computation of the prefactor of the cubic term to the next order in τ . We will argue that the cubic behavior is generic in models with continuous replica symmetry breaking, and use numerical simulations to substantiate this scenario.

In order to compute $\Delta F(q)$ one has to replicate n times both the spins σ_i and the spins τ_i . Two order parameter matrices appear:

$$Q_{ab} = \langle \sigma_a \sigma_b \rangle = \langle \tau_a \tau_b \rangle \quad \text{and} \quad P_{ab} = \langle \sigma_a \tau_b \rangle \quad , \quad a, b = 1, \dots, n . \quad (3)$$

One makes a Parisi Ansatz [2] for both Q and P , introducing two functions $q(x)$ and $p(x)$. We now recast the two $n \times n$ matrices into a single $2n \times 2n$ matrix

$$\mathbf{Q} = \begin{pmatrix} Q & P \\ P & Q \end{pmatrix} . \quad (4)$$

Let us consider in all generality any system that is described in the uncoupled case by the free energy functional $F[Q]$ in terms of the usual replica matrix. The same system when coupled according to (2) has a free energy functional of the form

$$F_2[Q, P] = F[\mathbf{Q}] + \epsilon(nq - \sum_{a=1}^n P_{aa}) , \quad (5)$$

where ϵ is a Lagrange multiplier associated to the δ -function in (2).

If the problem of a single, uncoupled, system admits a continuous solution $q_F(x)$ (what we suppose to be known), it is known that the corresponding variational equations related to the coupled problem admit two simple solutions [9].

A first solution has $\Delta F = \epsilon = 0$, and the functions $q(x)$ and $p(x)$ can be constructed explicitly from $q_F(x)$:

$$q(x) = \begin{cases} q_F(2x) & 0 \leq x \leq \frac{\tilde{x}}{2} \\ q & \frac{\tilde{x}}{2} \leq x < \tilde{x} \\ q_F(x) & 1 \geq x \geq \tilde{x} \end{cases} \quad p(x) = \begin{cases} q_F(x) & 0 \leq x \leq \tilde{x} \\ q & \tilde{x} \leq x < 1 \end{cases}, \quad (6)$$

where the point \tilde{x} is defined by the relation $q_F(\tilde{x}) = q$.

In the second solution $q(x) = p(x)$. This second solution becomes degenerate with the first one at $q = q_{EA}$. If we take the usual attitude one takes in the replica approach, i.e. that for $n \rightarrow 0$ we have to *maximize* the free energy with respect to the Q -parameters (and in agreement with the physical intuition about the problem) we will select the first solution in the region with $q < q_{EA}$ (where it has a larger free energy) and the second one in the region with $q > q_{EA}$, where it has a larger free energy.

Notice that while the first solution has a flat free energy $\Delta F(q) = 0$, the second, as a consequence of the facts that

1. it coincides with the first one for $q = q_{EA}$;
2. it has to be a solution of the saddle point equations;

must be such that $\frac{d\Delta F(q)}{dq}|_{q=q_{EA}} = 0$. All these properties together imply that generically $\Delta F(q) = \mathcal{A}(q - q_{EA})^3$, where \mathcal{A} is a problem dependent, temperature dependent, constant. Of course the accidental vanishing of \mathcal{A} is an allowed possibility, and in that case $\Delta F(q)$ would be of order five or higher.

Let us now turn to the explicit computation for the SK model close to T_c . In this case the replica free energy can be written as

$$F_2[Q, P] = \tau \operatorname{Tr} \mathbf{Q}^{*2} + \frac{1}{3} \operatorname{Tr} \mathbf{Q}^{*3} + \frac{1}{4} y \sum_{\alpha, \beta}^{1, 2n} \mathbf{Q}_{\alpha, \beta}^{*4} + \epsilon(nq - \sum_{a=1}^n P_{aa}^*), \quad (7)$$

where $y = \frac{2}{3}$, but it is convenient to keep it as a parameter during the computation, and we have defined $Q_{ab}^* \equiv Q_{ab}/T^2 \simeq Q_{ab}(1 + 2\tau)$ and $P_{ab}^* \equiv P_{ab}/T^2$. Here the solution can be found explicitly.

In fact, writing $\tilde{p}^* = P_{aa}^*$ and inserting $P_{ab}^* = Q_{ab}^*$ ($a \neq b$) in the equation of motion one finds that the matrix Q^* verifies the equation:

$$(\tau + \tilde{p}^*)Q_{ab}^* + (Q^{*2})_{ab} + \frac{y}{2} Q_{ab}^{*3} = 0, \quad (8)$$

which is identical to the solution of the free problem with $\tau \rightarrow (\tau + \tilde{p}^*)/2$ and $y \rightarrow y/2$. Plugging then the known solution into the free energy functional it is easy to derive the result:

$$\Delta F(q) = \left(\frac{1}{6} - \frac{3}{4}\tau y\right)(q^* - q_{EA}^*)^3. \quad (9)$$

Or, using the original definition of q , and $y = \frac{2}{3}$,

$$\Delta F(q) = \left(\frac{1}{6} + \frac{1}{2}\tau\right)(q - q_{EA})^3. \quad (10)$$

Let us now discuss the paramagnetic phase, where $T > T_c$. Here $q_{EA} = 0$ and we have to select the solution that has always $p(x) = q(x)$ for $q \geq 0$ and $p(x) = -q(x)$ for $q < 0$. Let us consider the replica symmetric free energy, corresponding to $\tilde{p} = q$, $q(x) = \text{sgn}(q)$, $p(x) = q_0$. For simplicity we will write as before equations valid for $q > 0$, keeping in mind that the free energy $F(q, T)$ has to satisfy $F(-q, T) = F(q, T)$.

Defining $Dy = \frac{e^{-\frac{1}{2}y^2}}{\sqrt{2\pi}}dy$, standard manipulations lead to

$$\begin{aligned} F(q, T) &= -\frac{\beta}{2}(1 + q^2 + 2q_0^2 - 2q_0 - 2qq_0) - T \log 2 + T\nu q \\ &\quad - T \int Dy \log [e^{-\nu} + e^\nu \cosh(2\beta\sqrt{q_0}y)] , \end{aligned} \quad (11)$$

that has to be extremized with respect to q_0 and ν (the Lagrange multiplier associated to q). This leads to the saddle point equations

$$q = \int Dy \frac{-e^{-\nu} + e^\nu \cosh(2\beta\sqrt{q_0}y)}{e^{-\nu} + e^\nu \cosh(2\beta\sqrt{q_0}y)} \quad (12)$$

$$q_0 = \frac{1+q}{2} - \frac{1}{2\beta\sqrt{q_0}y} \int Dy \frac{ye^\nu \sinh(2\beta\sqrt{q_0}y)}{e^{-\nu} + e^\nu \cosh(2\beta\sqrt{q_0}y)}. \quad (13)$$

These equations have always the trivial solution $q_0 = 0$, $\nu = \tanh^{-1} q$, which is correct at high enough temperatures and small values of q . A small q_0 expansion reveals that a solution with $q_0 \neq 0$ is possible for $q \geq T - 1 = q_c(T)$. Notice that

- for $T \leq 1$ the solution is non-trivial for all values of q ,
- for $T > 2$ the solution is always $q_0 = 0$,
- for $1 < T \leq 2$ there is a phase transition from $q_0 = 0$ for $q < T - 1$ to a solution $q_0 \neq 0$ for $q > T - 1$.

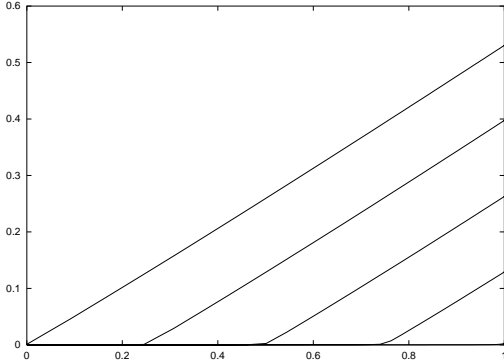


Figure 1: The induced overlap q_0 as a function of the mutual overlap q that we force on the system for $T = 1.0, 1.25, 1.5, 1.75$ and 2.00 (from right to left). Note that for $T = 1$ $q_0 = 0 \forall q$.

The correct solution in this last domain should break the replica symmetry. Close to $q_c(T)$ a small q expansion as in the previous section can be used even for large values of $T_c - T$. For $q_c(T) - q \approx 1$ we only consider the replica symmetric approximation. It is clear that if we impose $q = 1$ the system behaves as a single system with temperature $T/2$, and we understand therefore why $q_c(2) = 1$.

The $q_0 = 0$ solution gives a free energy

$$F(q, T) = -\frac{\beta}{2}(1 + q^2) - 2T \log 2 + T\nu q - T \log[\cosh(\nu)] . \quad (14)$$

In figure (1) we show the solution for q_0 as a function of q . For $q = 1$ we find that q_0 takes, as it should, the value of $q_{RS}(T/2)$, i.e. the Edwards–Anderson value at temperature $T/2$ in the RS approximation. The functional form of q_0 is well approximated for all values of T by $q_0(q) = q_{RS}(\frac{T}{2})(q - q_c(T))$, although small quadratic deviation from this form are observable. In figure (2) we also plot the related free energy.

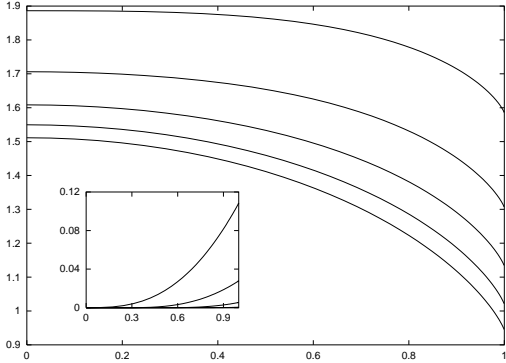


Figure 2: The free energy $-\beta F(q)$ for the same values of the temperature as in figure 1 (from top to bottom). In the insert we plot the difference $-\beta(F_0(q) - F(q))$ again for the same temperature values of figure 1, where $F_0(q)$ is computed with the trivial solution $q_0 = 0$ (from top to bottom. The difference is zero for $T = 2$ and very small for $T = 1.75$).

3 Numerical Results versus Analytic Solution

In the following we will use some numerical results obtained from simulations of the SK model toward two different goals, that we have already partially discussed in the introduction. First we want to have a numerical check of our analytical findings: it is clear that we are dealing with complex set of equations, we are working in some asymptotic regimes, and that this implies that a numerical check is welcome. The second issue is maybe less direct but also very crucial. It is important to understand how well numerical simulations done on finite lattice encompass the infinite volume physics, and, at the same time, how good a control we can have on the temperature range that we explore. The issue of the infinite volume limit is indeed of very large importance, and it is crucial to verify that exotic phenomena (like the large deviation regime we are discussing here) are already well quantified in the region of lengths we can study with nowadays computer facilities.

Our large scale numerical simulations are based on the numerical optimized Monte Carlo technique of the *parallel tempering* [10]. They have been run on parallel computer, and are essentially the same used

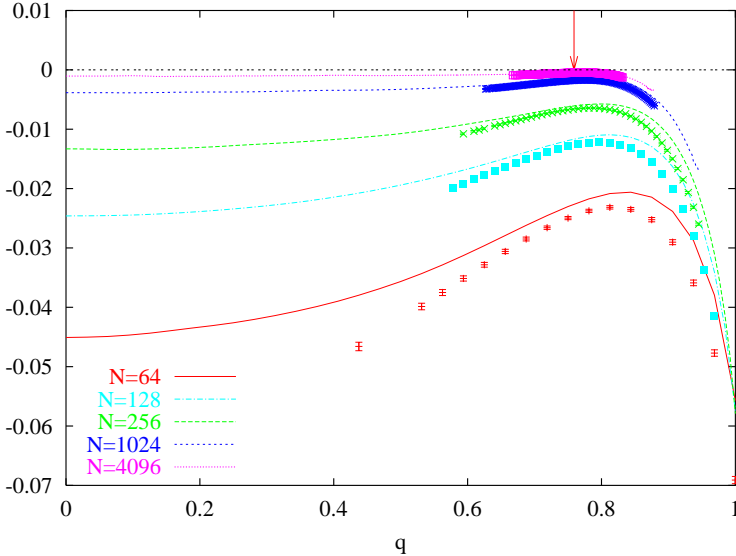


Figure 3: $\frac{1}{N} \log (P_N(q) N^{-\frac{1}{3}})$ versus q for $T = 0.4$: annealed ($F(q)$, represented by lines) and quenched ($\tilde{F}(q)$, represented by points with error bars) estimates. The vertical arrow indicates the value of q_{EA} at $T = 0.4$.

in [6] (but for the addition of the data obtained on a $N = 128$ site lattice).

We have analyzed 1024 different disorder realizations for $N = 64$, 256, 1024 and 4096 sites, and 8192 samples for $N = 128$. We go down to a minimal temperature value $T_m = 0.4$ $T_c = 0.4$, and we use $0.4 \cdot 10^6$ iterations for thermalizing and 10^6 iterations for measurements. We normalize probability distributions according to $\int_{-1}^1 P_N(q) dq = 1$.

The first question we discuss is whether it is appropriate to measure the quenched average

$$\frac{\Delta \tilde{F}(q)}{T} = N^{-1} \overline{\log P_{N,J}(q)} \quad (15)$$

(that is the quantity computed using the two-replica method) or if we can be happy by measuring the annealed average

$$\frac{\Delta F(q)}{T} = N^{-1} \log \overline{P_{N,J}(q)} \quad (16)$$

(a quantity that is much easier to measure with Monte Carlo simulation). In section 2 we have discussed the issue, arguing that these two

averages could differ because of rare samples: to be sure of that we analyze now our numerical data.

In figure 3 we show results for both the quenched (15) and the annealed (16) averages at $T = 0.4$ as a function of q . We plot data for $N = 64, 128, 256$ and 1024 . In order to make the figure readable:

1. we have subtracted to the different measurements a term $\frac{1}{3} \log N$ (this separates the points from different system sizes);
2. we have not drawn the $F(q)$ data as points with statistical error bars, but we have only drawn a line through the data points.

The (few) data points for $\tilde{F}(q)$ are drawn with statistical error bars (estimated from the variance of sample to sample fluctuations). It appears that the data for $\tilde{F}(q)$ are confined to a much smaller q range than the data for $F(q)$. This is expected since for a given value of q , $\tilde{F}(q)$ is well defined only if (the estimate of) $P_N(q)$ is larger than zero for every sample, whereas $F(q)$ is well defined as soon as the average $P_N(q)$ is larger than zero.

Figure 3 shows that for large system sizes the annealed and quenched estimates are consistent. The same conclusion holds for all the other values of the temperature that we have considered. Because of that in what follows we will only consider the annealed averages $P_N(q)$ and $F(q)$. We will estimate statistical errors on our observables by a jack-knife procedure [11].

Our second (and main) numerical goal is in trying to verify the predictions of equation 10: we asymptotically expect a cubic behavior of $\frac{1}{N} \log P_N(q)$ in $q - q_{EA}$, with a leading prefactor that we have computed in 10. Now, is all that correct? Can we already observe this behavior on the lattice size where we are able to thermalize the system in the spin glass phase?

We report our results at different values of the temperature ($T = 1.0, 0.8, 0.6$ and 0.4) respectively in figures 4, 5, 6 and 7. With the dotted line (the upper one where we have two lines, see later) we plot the theoretical prediction of equation 10. With an horizontal arrow we give the analytic value of $P_N(q = 1)$ (see the discussion later on).

All figures show that results for the systems of different sizes are converging to a common (N independent) function: our results for the excess free energy are indeed in the asymptotic regime. The careful reader will notice that only the limit $\lim_{N \rightarrow \infty} 1/N \log P_N(q)$ is predicted. There is accordingly an order $1/N$ ambiguity in the vertical offset of our plots for $1/N \log P_N(q)$.

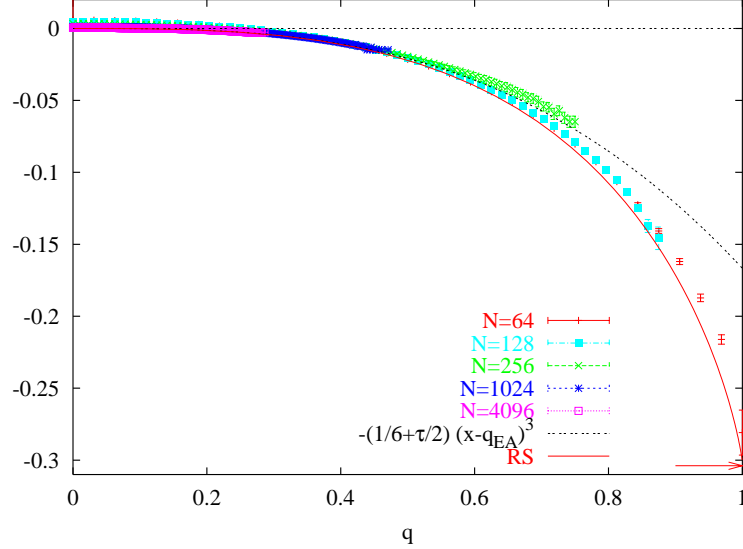


Figure 4: $\frac{1}{N} \log P_N(q)$ versus q for $T = 1$: points with error bars are for numerical data from different lattice sizes, the dotted line is from the perturbative estimate in the spin glass phase. An horizontal arrow indicates the exact $q = 1$ value. The full line (labeled “RS”) is from equation 11.

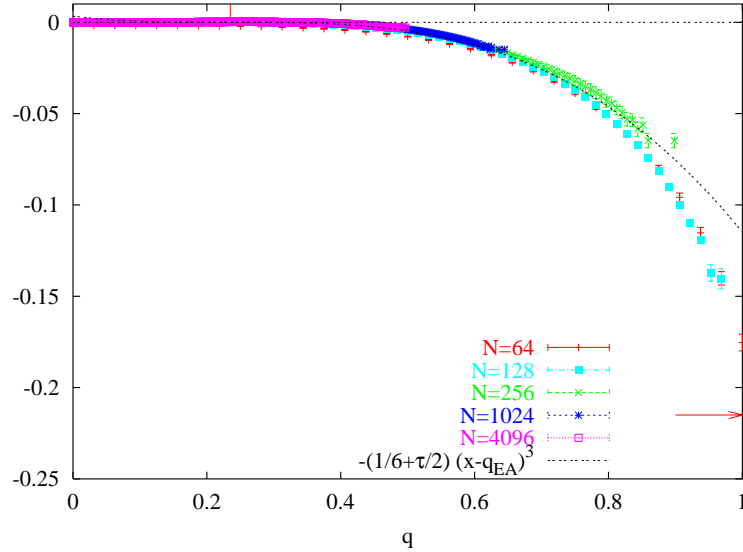


Figure 5: As in figure 4 but with $T = 0.8$. The additional vertical arrow indicates the value of q_{EA} .

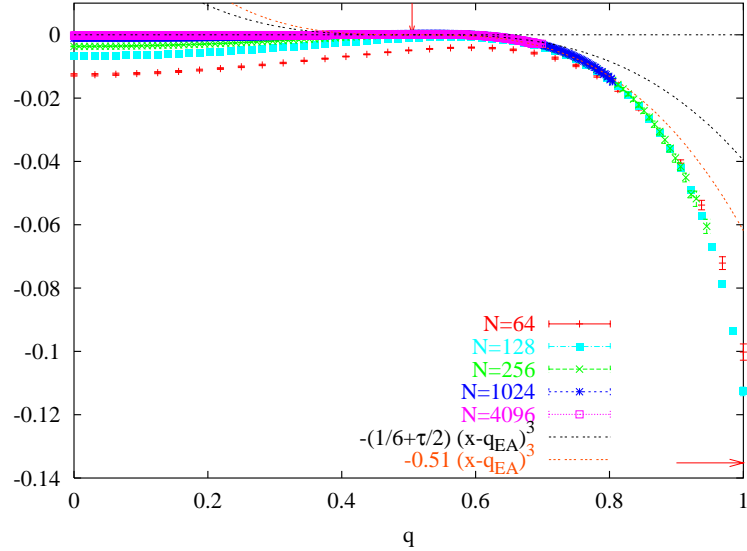


Figure 6: As in figure 4 but with $T = 0.6$. The additional lower dotted curve is drawn by using a coefficient modified by hand, accounting for the renormalization of the temperature when τ grows.

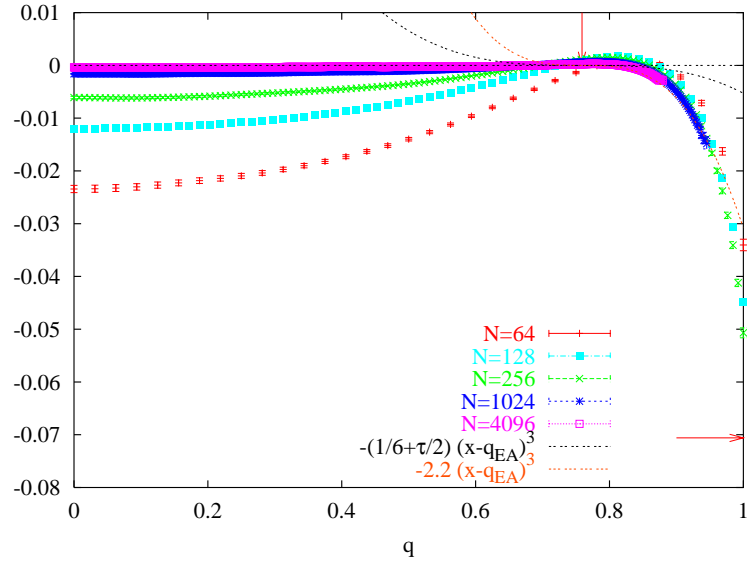


Figure 7: As in figure 6 but with $T = 0.4$.

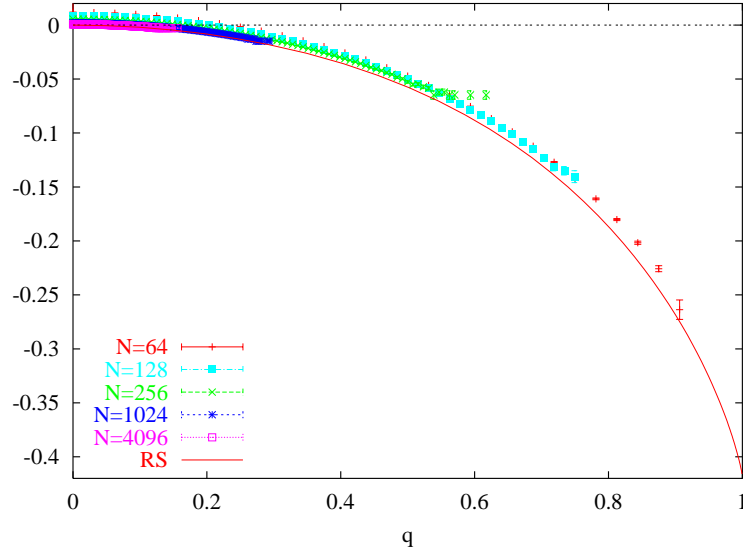


Figure 8: As in figure 6 but with $T = 1.3$.

At $T = 1$, where $q_{EA} = 0$, the agreement of our data with the theoretical prediction is very good at least up to $q = 0.6$. Also at $T = 0.8$, where q_{EA} is slightly larger than 0.2 (i.e. still very small) the agreement is very good in a very large q range (up to $q \simeq 0.8$).

At $T = 0.6$, where q_{EA} is of order 0.5 and a small τ expansion starts to be partially inappropriate, the agreement starts to be less good. To take into account the fact that here τ is large and there is an effective renormalization (the first order correction in equation 10, equal to $\frac{1}{2}\tau$, at $T = 0.6$ is of the same order than the leading term, $\frac{1}{6}$) we have added a further curve where we substitute the prefactor we have computed analytically in equation 10 with some effective value, that optimizes the matching of the analytic form to the numerical data: this improves very much the agreement. This effect is even more dramatic at $T = 0.4$: still, preserving a cubic dependence with a renormalized prefactor fits very well the data in a large $q > q_{EA}$ range. In all these analysis we have used the value of q_{EA} computed by Crisanti and Rizzo by numerical integration [12] of the Parisi solution of the SK model (we have never used q_{EA} computed to order τ).

Our third numerical point concerns the value of $P_N(q)$ at $q = 1$ (that we plot with an horizontal arrow in the four figures). We use the estimate derived with high precision in [12] for the free energy of

the Parisi solution. We use the simple relation

$$\frac{1}{N} \log P_N(q = 1) = -\frac{2}{T} \left(F\left(\frac{T}{2}\right) - F(T) \right). \quad (17)$$

One sees from figures 4-7 that the prediction of 17 for $P_N(q = 1)$ is smaller than the value that formula 10 takes at $q = 1$: obviously this had to be expected, since equation 10 is the first term in an expansion in powers of $q - q_{EA}$, and is not supposed to be valid up to the $q = 1$ boundary, where higher orders cannot be neglected. Note however that the interplay between finite size effects and higher orders in $T_c - T$ is not trivial. It could be studied numerically using the multi-overlap algorithm [13] which allows to measure $P_N(q)$ with high accuracy up to $q = 1$. Parallel tempering numerical data, when pushed to very high statistics, confirm already in a remarkable way the analytic value: this can be only done for small lattice sizes. At $T = 1$ we are able to push the $N = 64$ lattice up to $q = 1$ and to keep under control the limit of the $N = 128$ lattice. At lower T values the check is slightly more difficult, but one sees that the $q = 1$ limit of larger and larger lattices approaches better and better the analytic value.

That the situation is well under control can be shown nicely for $T \geq 1$ by comparing the numerical data, in the whole $q \in [0, 1]$ range, with the results of our RS computation of equation 11. This is done in figures 4 for $T = 1.0$ and 8 for $T = 1.3$ (the highest temperature alas in our parallel tempering simulation). The first figure shows the full line (labeled “RS”) cleanly overshooting the dotted line, to reach the $q = 1$ axis slightly above (as expected) the exact $q = 1$ limit. Figure 8 show also again the agreement our our numerics with the replica calculation.

Equation 10 suggests [7], [8] that (for $T < T_c$) asymptotically $P_N(q)$ scales as

$$P_N(q) N^{-\frac{1}{3}} = \mathcal{F}\left(N(q - q_{EA})^3\right) \quad \text{for } q > q_{EA}, \quad (18)$$

with $\mathcal{F}(z) \propto \exp(-Az)$, with some positive constant A , for large z . If the above formula holds down to the maximum of $P_N(q)$ this implies that the location of the peak of the probability distribution of the overlap on a lattice of size N , that we denote by $q_{max}(N)$, has to behave like

$$q_{max}(N) = q_{EA} + cN^{-\frac{1}{3}},$$

a behavior that has been verified with high accuracy in older work [6].

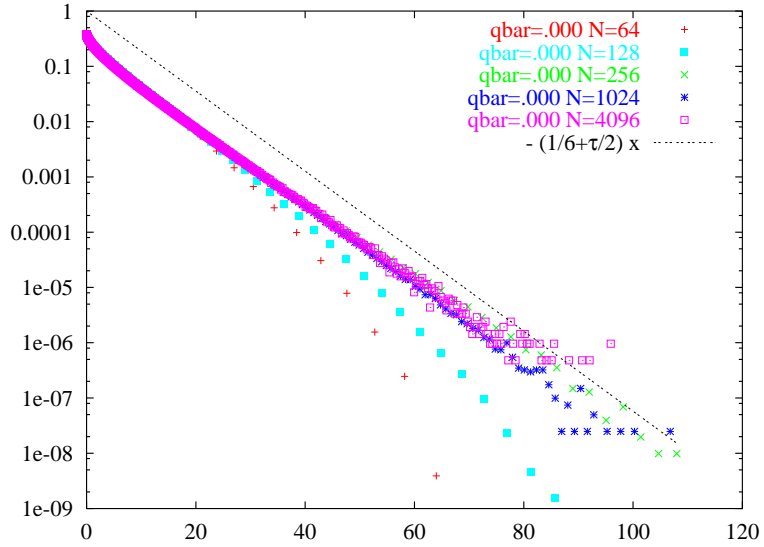


Figure 9: Scaling plot of $P_N(q) N^{-\frac{1}{3}}$ as a function of $(q - q_{max}(N))^3 N$ for $T = 1.0$, compared with the coupled replica estimate (with arbitrary normalization). Our estimate of $q_{max}(N)$ is reported in the figure under the name **qbar** (it is obviously zero at T_c) .

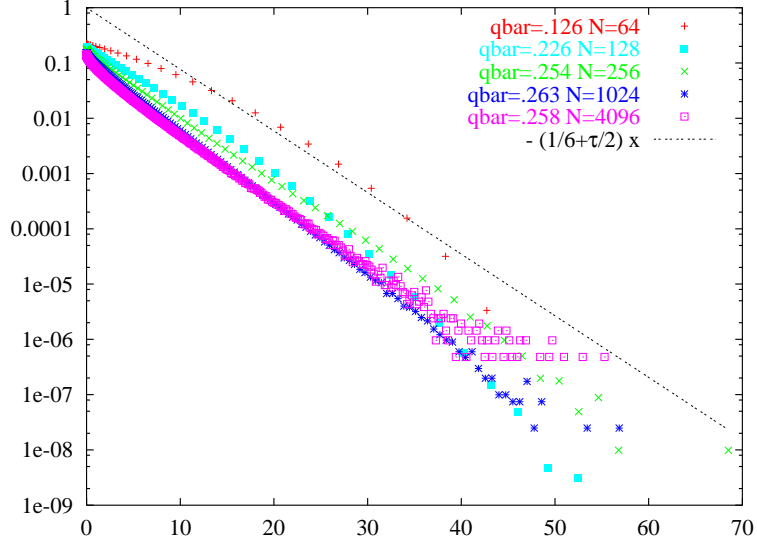


Figure 10: As in figure 9 but for $T = 0.8$. Note that $q_{max}(N)$ is not well defined on small systems at this temperature, that is close to T_c .

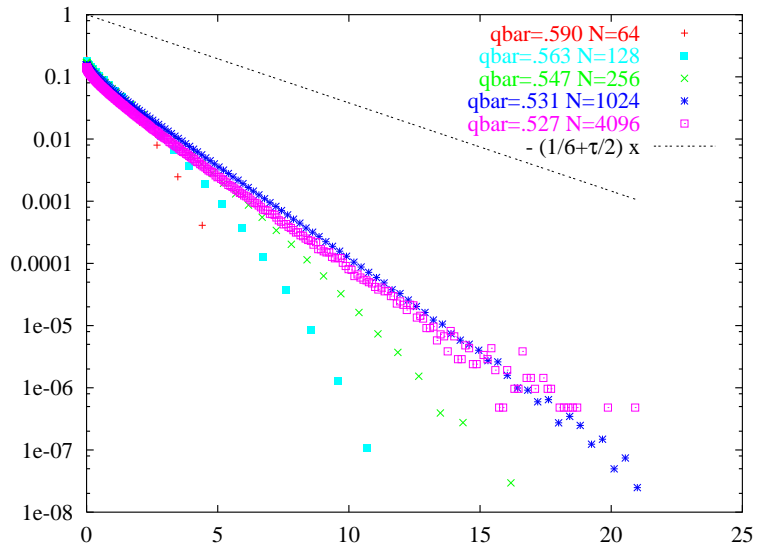


Figure 11: As in figure 9 but for $T = 0.6$.

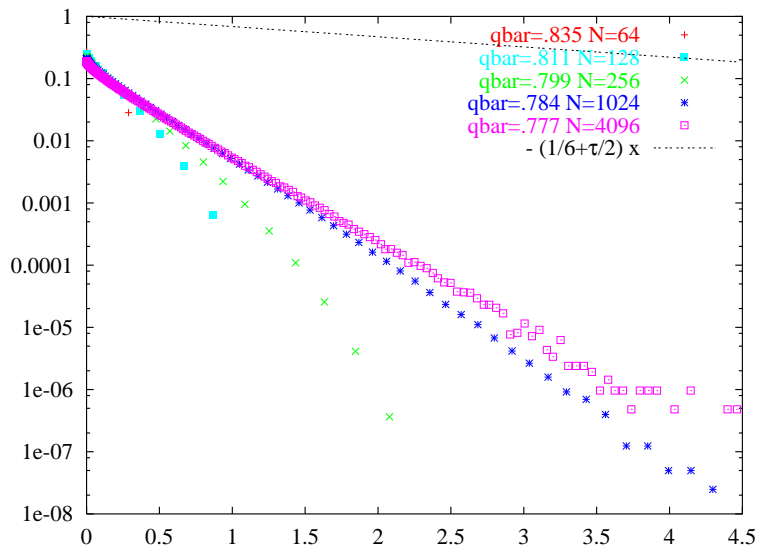


Figure 12: As in figure 9 but for $T = 0.4$.

In what follows we will accordingly look for a scaling law in the form

$$P_N(q) N^{-\frac{1}{3}} = \mathcal{G} \left(N(q - q_{max}(N))^3 \right) \quad (19)$$

using the numerical data obtained for $q_{max}(N)$. Figures 9, 10, 11 and 12, are scaling plots of $\log P_N(q) N^{-\frac{1}{3}}$ versus $N(q - q_{max}(N))^3$. The figures clearly exhibit the predicted cubic behavior.

It should be stressed that with our data scaling in $(q - q_{max})^3 N$ is much better than scaling in $(q - q_{EA})^3 N$, using the very precise data for q_{EA} by Crisanti and Rizzo. It is indeed to be expected that if one uses a value of q_{EA} quite off from the true one³ the resulting scaling behavior is not good. One reason for this agreement is that for $q > q_{EA}$ the inflection point of $(q - q_{max})^3 N$ mimics with good accuracy the maximum of $\frac{1}{N} \log P_N(q)$.

4 Conclusions

The results of these analysis are very positive. We have first argued that the large deviation leading behavior of $P_N(q > q_{EA})$ in the Sherrington–Kirkpatrick model is generically $\frac{1}{N} \log P_N(q) = -\mathcal{A}(q - q_{EA})^3$, and we have computed the first corrections to the expansion of \mathcal{A} in powers of $T_c - T$.

Data from numerical simulations confirm that this behavior can be detected already on moderate lattice sizes. First we have seen that we are well allowed to take an annealed average of ΔF . Secondly we have analyzed the details of the cubic behavior, and checked the validity of the perturbative estimate of the prefactor: close to T_c it works very well, while far away from T_c a simple renormalization improves the agreement in a substantial way. Our very accurate data have allowed a detailed analysis of the $P(q = 1)$ value, allowing again for a positive check of the analytic result. For $T \geq T_c$ an exact computation in the replica symmetric scheme shows nicely the crossover from the $q \approx q_{EA}$ behavior to the ultimate limit $q = 1$. At last we have shown that the scaling plots for $P_N(q)$ improve appreciably if one uses $(q - q_{max})^3 N$ as the scaling variable, showing clearly the predicted cubic behavior of $\log P_N(q) N^{-\frac{1}{3}}$.

³Scaling plots as function of an ad-hoc N independent q_{EA} appear (in a small q interval) in [7] for $T = 0.8$, and in [8] for $T = 0.5$.

Acknowledgments

We thank A. Crisanti and T. Rizzo for providing us with their unpublished numerical evaluations of quantities in the SK model. SF thanks the SPhT Saclay for a visiting professor fellowship and warm hospitality in the months of October-December 2001, during which part of this work was performed.

References

- [1] G. Parisi, Phys. Rev. Lett. **43** (1979) 1754.
- [2] M. Mézard, G. Parisi, and M.A. Virasoro, *Spin Glass Theory and Beyond* (World Scientific, Singapore, 1987).
- [3] S. Franz, G. Parisi and M. A. Virasoro, J. Phys. I (France) **2** (1992) 1869.
- [4] N. D. MacKenzie and P. Young, Phys. Rev. Lett. **49** (1982) 301; A. Billoire and E. Marinari, J. Phys. A **34** (2001) L1.
- [5] See for example A. Billoire and E. Marinari, J. Phys. A **33** (2000) L265, and references therein.
- [6] A. Billoire and E. Marinari, preprint cond-mat/0202473.
- [7] G. Parisi, F. Ritort and F. Slanina, J. Phys. A **26** (1993) 3775.
- [8] J.C. Ciria, G. Parisi, and F. Ritort, J. Phys. A **26** (1993) 6731.
- [9] S. Franz, *PhD Thesis*, unpublished.
- [10] For an introduction see for example E. Marinari, in *Advances in Computer Simulations*, edited by J. Kerstz and I. Kondor (Springer-Verlag, Berlin 1998), p.50, preprint cond-mat/9612010.
- [11] H. Flyvbjerg, in the same book of reference [10].
- [12] A. Crisanti and T. Rizzo, preprint cond-mat/0111037 and private communication.
- [13] B. Berg, A. Billoire and W. Janke, Phys. Rev. E **65** (2002) 045102R, preprint cond-mat/0108034; preprint cond-mat/0205377.